Received: 10 October 2022 | Revised: 29 November 2022 | Accepted: 4 January 2023

DOI: 10.1002/ima.22849

RESEARCH ARTICLE

WILEY

Image processing and machine learning-based bone fracture detection and classification using X-ray images

Muhammet Emin Sahin

Department of Computer Engineering, Yozgat Bozok University, Yozgat, Turkey

Correspondence
Muhammet Emin Sahin, Department of Computer Engineering, Yozgat Bozok University, Yozgat, Turkey.
Email: emin.sahin@bozok.edu.tr

Abstract

One of the most important problems in orthopedics is undiagnosed or misdiagnosed bone fractures. This can lead to patients receiving an incorrect diagnosis or treatment, which can result in a longer treatment period. In this study, fracture detection and classification are performed using various machine learning techniques using of a dataset containing various bones (normal and fractured). Firstly, the X-ray images obtained are subjected to image preprocessing stages and are prepared for the feature extraction stage. Then, in addition to the Canny and Sobel edge detection methods used in the image processing stage, feature extraction of X-ray images is performed with the help of Houhg line detection and Harris corner detector. The data obtained by performing feature extraction is given to 12 different machine learning classifiers and the results are presented. Setting hyperparameters for classifiers is done by the grid search method, and the study is tested for 10-fold cross-validation. Classifier results are presented comparatively as accuracy, training time, and testing time, and linear discriminant analysis (LDA) reaches the highest accuracy rate with 88.67% and 0.89 AUC. The proposed computer-aided diagnosis system (CAD) will reduce the burden on physicians by identifying fractures with high accuracy.

KEYWORDS

bone fracture, classification, feature extraction, image processing, machine learning, X-ray images

1 | INTRODUCTION

Bones, which are composed of organic/inorganic materials and have a durable structure, are the most important organism in providing the body's support. Bone, which has a light structure as well as sensitive, can crack or break when exposed to excessive force. Apart from osteoporosis, reasons such as falls, sports injuries, and traffic accidents can cause bone fractures. Today, with the development of medical device technologies, bone fractures can be detected by using devices such as X-ray and computed tomography (CT). Doctors or radiologists diagnose whether the bones are broken by examining the X-ray images obtained. However, it can be misdiagnosed in difficult-to-identify fracture or crack detection, and as a result, both doctors and patients can be in a difficult situation. In recent years, many studies in the field of biomedicine have focused on computer-aided diagnostic systems to facilitate the detection of various diseases. Advances in artificial intelligence also show that deep learning architectures have the capacity to diagnose at the level of healthcare professionals.[1–6] Machine learning methods have been widely used in the field of medicine in recent years and many studies have been presented in the literature.[7–9]

In real life, radiologists and physicians usually transmit x-rays to determine if a fracture is present and what type of fracture it is specifically. For the purpose of detecting fractures, manual inspection or a traditional X-ray system should be used. The computer vision system can help scan X-ray images for suspected cases and alert doctors. According to related studies, fractures in CT or X-ray images can be classified with high precision using new algorithms that have entered the literature.[10–12] Depending on the type of bone, there are different studies in the literature. It is possible to divide these studies into two categories: studies using machine learning and deep learning methods. Studies using machine learning methods are based on preprocessing and classification steps. In the preprocessing step, various image processing techniques are used to remove noise from images. In the classification step, features must be extracted from the images to support the classifier to be used. Support Vector Machine (SVM), Naïve Bayes (NB), artificial neural networks (ANN or NN), decision trees (DT), and random forest (RF) are widely used classifiers for fracture detection and classification.

Olczak et al. performed a study on fracture detection on radiographs of various body parts.[4] The images include ankle, wrist, and hand regions. According to these experiments, the VGG-16 ready architecture achieved 99%, 95% and 90% performance for the classification and detection problems, respectively, over the overall accuracy performance criterion. Avinash et al. performed a fracture-type determination study on X-ray images of the humerus, ulna, femur, tibia, and fibula.[13] In the preprocessing phase, the Canny edge detection and Harris corner detector algorithms are applied to the images. In the feature extraction stage, the bag of words (BoW) model used in the text classification problem was chosen. SVM was used as a classifier in the study, and the performance of the system was calculated as 78% according to the results of the 10-fold cross-validation method. Bayram and Çakıroğlu performed a study to classify diaphyseal femur fractures using X-ray images.[14] It identifies nine types of fractures in the classification process. The dataset includes 196 femoral images. It has been shown that the SVM classifier is superior to other classifiers with a score of 89.87% in the performance evaluations made on the general accuracy performance criterion using 10-fold cross-validation tests. Tripathi et al. performed a study for fracture detection on X-ray images of the femur.[15] In the preprocessing stage, firstly, noise removal was applied to the images with the mean filter and median filter methods. In the study in which the SVM classifier was used, the performance of the system was measured at 87.5% over the general accuracy criterion. Basha et al. performed a fracture detection study on long bones using X-ray images.[16] *In their study, 60 of the 80 images containing fractures were reserved for training and 20 for testing*. It has been reported that the NN (RBFNN) classifier using radial-based function has passed the performances of Hough transform-based fracture detection (HTBFD) and kNN classifier with 88% performance over the overall accuracy performance criterion. Guan et al. tried to determine the location of arm fractures from X-ray images.[17] In their previous work,[18] they modified the CNN architecture and applied it to X-ray images containing arm fractures. The performance of the proposed system was measured at 62.04%, based on the average precision performance criterion.

In this study, image preprocessing steps are applied for fracture detection, and the images that have feature extraction are classified with different classifiers. It is of great importance in terms of performing feature extraction and doing this with a large number of machine learning algorithms. In this paper, 12 machine learning algorithms, which are logistic regression, linear discriminant analysis (LDA), multi-layer perceptron (MLP) classifier, multinomial naive bayes, gaussian naive bayes, gradient boosting classifier, quadratic discriminant analysis, ada boost classifier, light gradient boosting machine classifier (LGBM), eXtreme gradient boosting (XGB) classifier, RF classifier, and extra trees classifier, are used on an experimental dataset. With the help of the grid search method, hyperparameters are found for machine learning classifiers. In addition, the reliability of the results obtained by performing the *k*-fold cross-validation process on the dataset is presented.

The following is an overview of the paper's structure. Section 2 briefly describes the algorithms and techniques commonly used in each, along with general steps such as image acquisition, data preprocessing, image segmentation, extraction of images, and bone fracture classification extraction of images, and bone fracture classification (automated bone fracture detection and classification using machine learning). Section 3 includes experimental work on machine learning classifiers, results, and evaluation metrics like accuracy, recall, precision, and F1-score. Discussion is given in Section 4. Finally, conclusions and suggestions for future investigation are presented in Section 5. An overview of the study is given in Figure 1.

2 | MATERIAL AND METHODS

In this study, the bone fracture detection system is implemented in four stages, which are image acquisition, image preprocessing, feature extraction, and classification stages, respectively. Typical computer-aided diagnostic

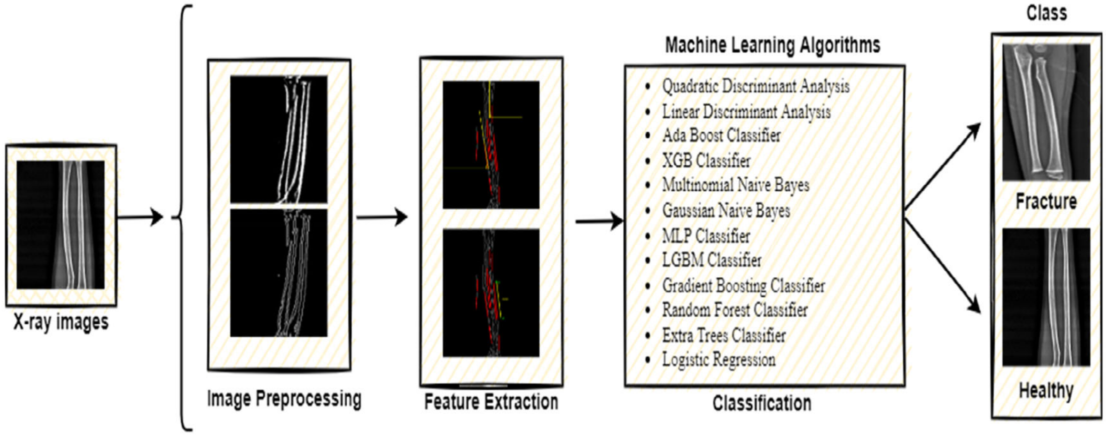

FIGURE 1 An overview of the study

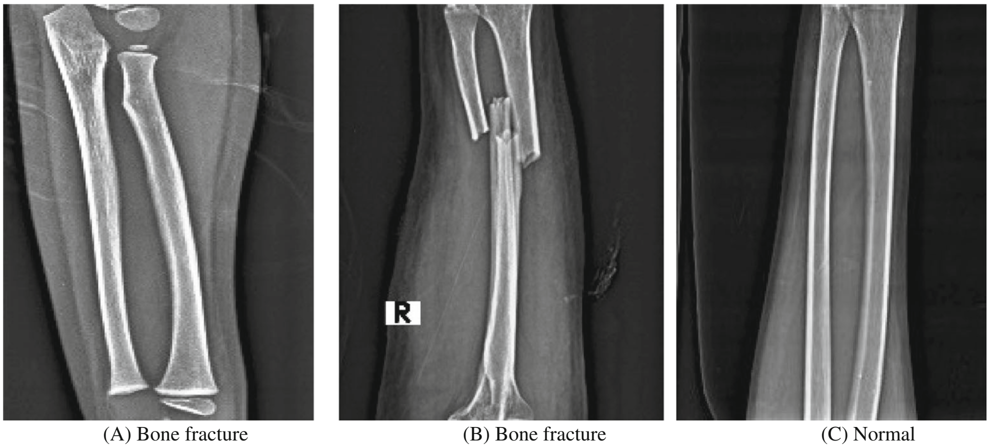

FIGURE 2 X-ray images (A) and (B) bone fractured (C) Normal cases

systems based on medical images include image processing tools for noise removal, enhancement, and feature extraction. X-ray images include normal and fractured bone images.

2.1 | Dataset

The data set used in this study was obtained as a dataset of X-ray images from Al-huda Digital X-ray Laboratory. It contains 105 normal and 71 fractured long bone images. There are different types of bone fractures: oblique, greeb-stick, comminuted, spiral, and transverse. This variety of data is available in the literature.[19] An example of X-ray images of bone is given in Figure 2. The data set includes images that is be used 70% for training and 30% for testing.

2.2 | Image preprocessing

In the image preprocessing stage, changes are made to the images by using various image processing techniques. The purpose of making these changes is to remove various disturbances such as noise from the image or to make the image better for the next stages such as segmentation and feature extraction. In this article, image processing is performed on Jupyter Notebook using python.

2.2.1 | Image acquisition

The images in the data set are in .jpg format and the images are in three-channel form. Each image read is converted to grayscale image format using color space conversion. Since the X-ray images used are single-channel, there is no loss of quality in the images.

2.2.2 | Thresholding

Thresholding methods are considered to be the simplest method of segmenting images. In such approaches, an image is usually converted to a binary image by defining a threshold. The image can be segmented using the boundaries of the resulting binary image. Thresholding is probably the most commonly used technique in image segmentation. Thresholding is applied to X-ray images in grayscale. With this process, pixels with gray values in certain ranges are changed to white (255 or 1) and all other pixels become black (0). The lower and upper values determined for the operation performed in this study are between 120 and 255. Here, pixels with values between 120 and 255 are determined to be white and other pixels to be black. The image formed after the thresholding process is transmitted to other processing steps at gray level.

2.2.3 | Edge detection

Edge detection is considered the most important operation in image processing. In most color images, edge detection is done by converting the images to grayscale. Edges in grayscale images can be defined as borders where the brightness levels of two regions are clearly different from each other. Edges are the most important information in the image.[20] Edge regions are also defined as the places where sudden changes in pixel values occur in images.

The Canny edge detection algorithm is one of successful the methods that finds changes in images and examines whether they are edges.[21] This method is a method developed by John F. Canny to find sharply defined edges on the image.[22] In the study, this method is used for image processing in the Opencv platform. The phase of highlighting the outer and inner edges of the bones in the image is performed.[23] The image obtained here is a bitwise image. In addition, the output obtained from here is used for finding the straight-line segment and the feature we call the perimeter in the next step.

Sobel, which is mainly used for vertical or horizontal edge detection, is used to detect edges with separate filters for both methods.[24] The part that distinguishes the Sobel method from the other edge detection method Canny for this study is that it can show an area closer to the area covered by the bones in the image as output.

2.2.4 | Hough line detection

The Hough transform is a method used for both line and circle detection.[25] The Hough line segment transform is used to detect straight lines in the given image. Since the algorithm can detect many lines, only 10 of the longest lines are detected and stored in memory for this study. These lines are then used for properties such as length and angle.

2.2.5 | Harris corner detector

Harris corner detector algorithm is generally used to detect corner points on the output obtained after edge detection.[26] In this study, this method, which is used in the process of distinguishing bone fractures, is applied to the images obtained from the Sobel edge detection process. The steps of the image pre-processing are shown in Figure 3.

2.3 | Feature extraction

Some features can be extracted from the digital images obtained after the image preprocessing step. Having more of these features means more features for classification, which can increase the classification accuracy. The features obtained in feature extraction can be derived from each other. Some of the features used are divided by the number of vertical pixels, and a kind of normalization is performed with the aim of making the features independent of the resolution of the image from which they are extracted. The properties obtained in this study to detect bone fractures are given below. The steps of feature extraction are shown in Figure 4.

2.3.1 | Perimeter (perimeter)

The perimeter feature is calculated as the number of white pixels, that is, determined edges, in the image obtained from the Canny edge detection algorithm. The obtained values are normalized by dividing by the number of vertical pixels.

2.3.2 | Area (area)

The area property is the number of white pixels obtained from the Sobel edge detection algorithm. As can be seen in the images obtained, it resembles the inner area of the bone with thick drawings. The value obtained here is proportional to the number of vertical pixels.

2.3.3 | Line, line length and average length (nm_lnslngth_pxl and avg_length)

This feature is obtained with the help of the Hough Lines algorithm. The Hough Lines algorithm gives the maximum number of line segments that can be drawn. Within the scope of this study, 10 lengths that we keep in memory are used in length and angle operations in the next steps.

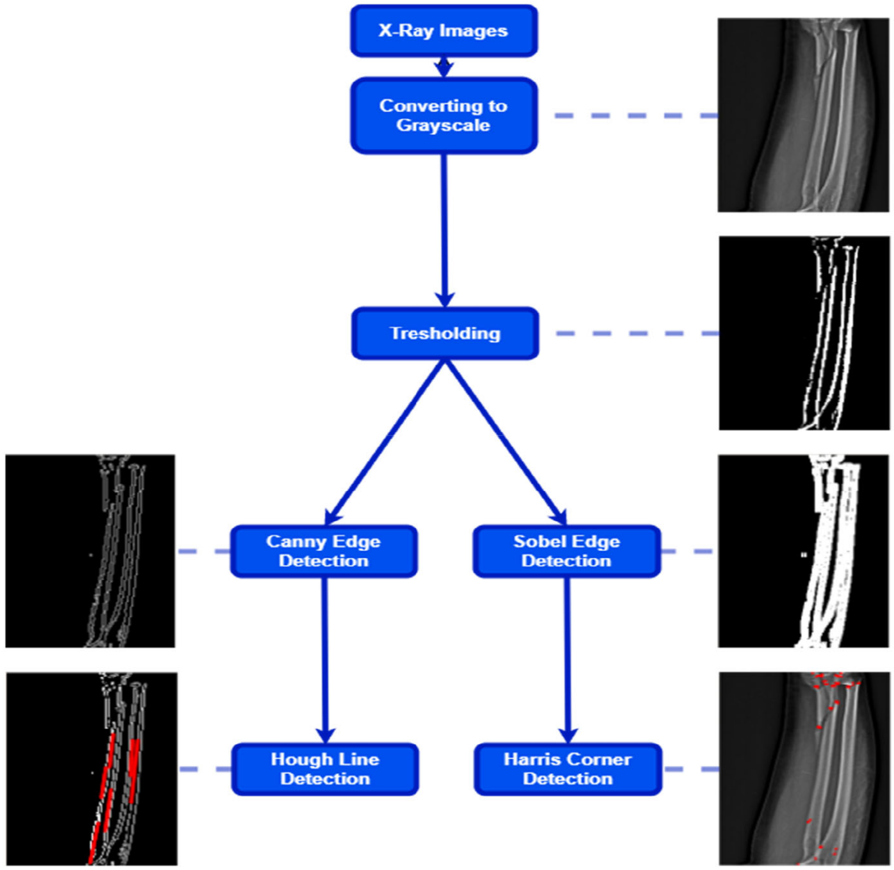

FIGURE 3 The steps of the image pre-processing

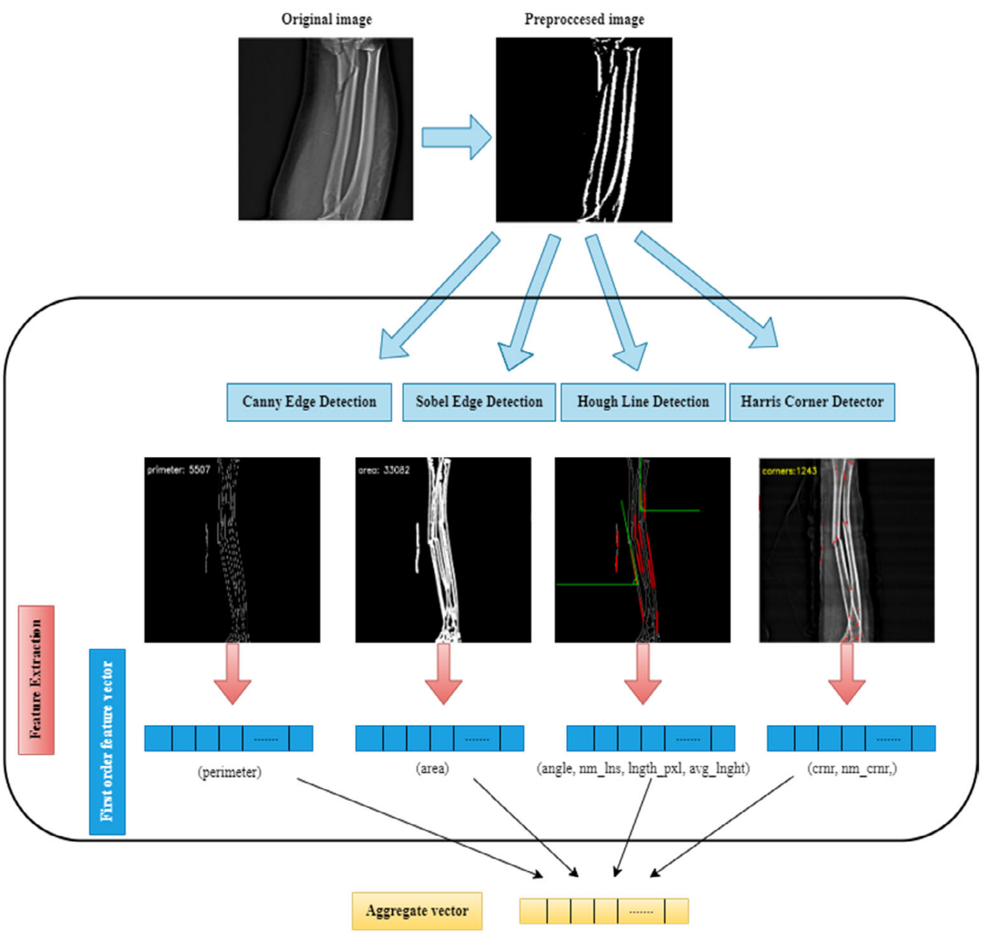

FIGURE 4 The steps of feature extraction

TABLE 1 Parameters

		Predicted	
		Negative	Positive
Actual cases	Negative	True negatives (*tn*)	True positives (*tp*)
	Positive	False negatives (*fn*)	False positives (*fp*)

2.3.4 | Slope (angle)

This feature, in which the maximum of the angles between the detected long line segments is calculated, is essentially based on the slope calculation. Two endpoints of the obtained line segment are used for the slope. Each slope calculation is made for 10 line segments. Then, the difference between the largest and smallest values among these 10 slope values is added to our data set as our angle value. There is also an important detail to note: the acute angle between two lines can be 90 degrees at most. If the value is greater than 90 degrees, the difference from 180 degrees should be calculated.

2.3.5 | Corner and total corner (crnt and nm_crnr)

With the result obtained from the Harris corner finding algorithm, the total number of corners is found. In addition, considering the ratio of the total number of vertices to the number of vertical pixels, two different features are obtained. A total of 8 features are obtained for the images in the data set and used within the scope of the study.

2.4 | Classification

Classification is basically a method by which certain decisions or predictions are made by learning and interpreting the available information and the data is divided into labels according to their characteristics. The classification task is used in a wide variety of fields. Machine learning uses various algorithms to solve problems. An algorithm cannot be said to be the most successful of all of the various problems. The successful algorithm changes according to the problems and data sets. The algorithm used varies depending on certain parameters such as the type of problem, the number of variables, and the type of model.[27] Within the scope of this study, the results are presented using 12 different machine learning algorithms for bone fracture detection.

2.5 | Evaluation methods

Different methods are used to measure the success of machine learning methods. Evaluation criteria are used to measure the accuracy, sensitivity, specificity, and F1-score of the system. Evaluation criteria are calculated over the confusion matrix, which includes correct and incorrect predictions as a result of classification. The confusion matrix is shown in Table 1.

Based on the results of Table 1, accuracy, sensitivity, specificity, precision, recall, and the F1-score are calculated and used in the evaluation of the results of this study.[28]

$$Accuracy = \frac{tn + tp}{tn + tp + fn + fp} \tag{1}$$

$$Recall = \frac{tp}{tp + fn} \tag{2}$$

$$Precision = \frac{tp}{tp + fp} \tag{3}$$

$$F1\_Score = 2 \times \frac{Precision \times Recall}{Precision + Recall} \tag{4}$$

3 | EXPERIMENTAL RESULTS AND DISCUSSION

In this study, bone fracture detection is classified using machine learning algorithms after the preprocessing feature extraction steps given above using the obtained dataset.

3.1 | Grid search

Hyperparameter fine-tuning can be done in the form of manual search, grid search, random search,[29] Bayesian optimization.[30] In this section, a comprehensive search and fine-tuning of all possible combinations of the specified hyperparameters is performed by Grid search and the obtained fine-tuned hyperparameter results are given.

3.2 | Cross-validation

A 10-fold cross-validation technique is applied to evaluate the classifier models. Cross-validation ensures that the class values at each fold are accurately represented. Therefore, it helps reduce the variance in the estimation. During this process, the samples are split into 10 (equally sized) sub-particles at random. One sub-sample from the total of 10 is kept to test the model, and the other 9 are used for training. The validation data is used once for each of the ten subsamples. A single estimate is generated by averaging the 10 results. As a result, all observations are used for both training and validation, with each observation only being used once for validation.[31] In our study, classification is performed with the 10-fold cross-validation method and the results are presented.

Correlation is often used to determine whether there is a cause and effect relationship between two variables. This value varies between −1 and 1. In the heatmap given in Figure 5, the relationship between the features and the classification label is presented. When the table is examined, it is seen that there is a high correlation between the *nm_crnr* attribute and the class label. This feature is followed by area and *crnr*, respectively. A scatter plot of the two variables is created and given in Figure 6. Because the dataset is contrived, there is a relationship between the two variables as shown in the figure.

The confusion matrix demonstrates the classification ratio's accuracy in the study. It shows how many of the data's observations are incorrect and how many are correctly categorized. Figure 7 shows the confusion matrix and classification reports for each classifier that are estimated on the testing data set and built using the study's training data. Accuracy, training and testing times are given in Figure 8.

The ROC curve is a graph of true positives rate (sensitivity) against the rate of false-positives. The ROC curve is frequently used as a performance evaluation tool for many different kinds of classification problems. The overall accuracy values are determined by the AUC values found in the ROC curve. It demonstrates the classification accuracy of the models used in the ROC curve. When evaluating the methods used in the ROC curve, it aids in determining the best model. The LDA classifier has the highest AUC value of 0.89 among the proposed classifiers when the ROC graph shown in Figure 9 is examined. With scores of 0.86 and 0.85, respectively, logistic regression and RF classifiers come in second and third. The accuracy of the study depends on having

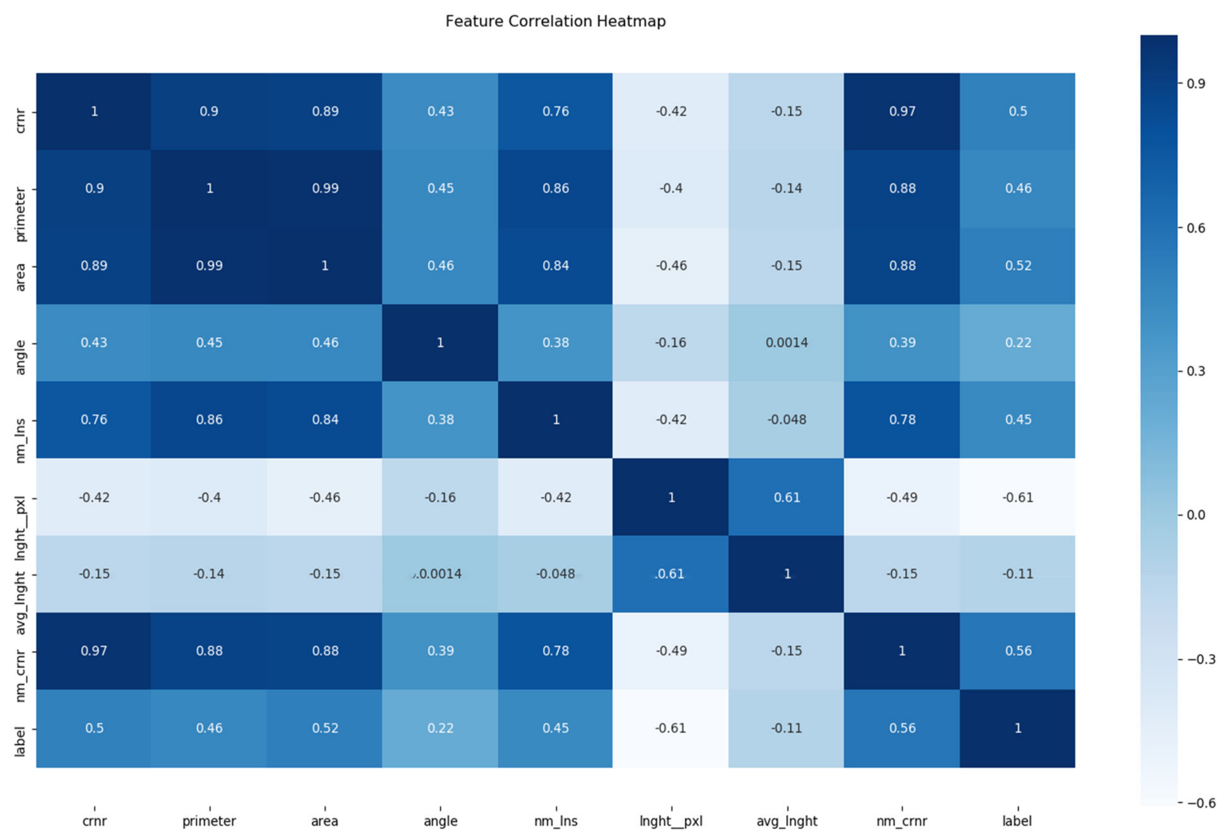

FIGURE 5 Heat map of features

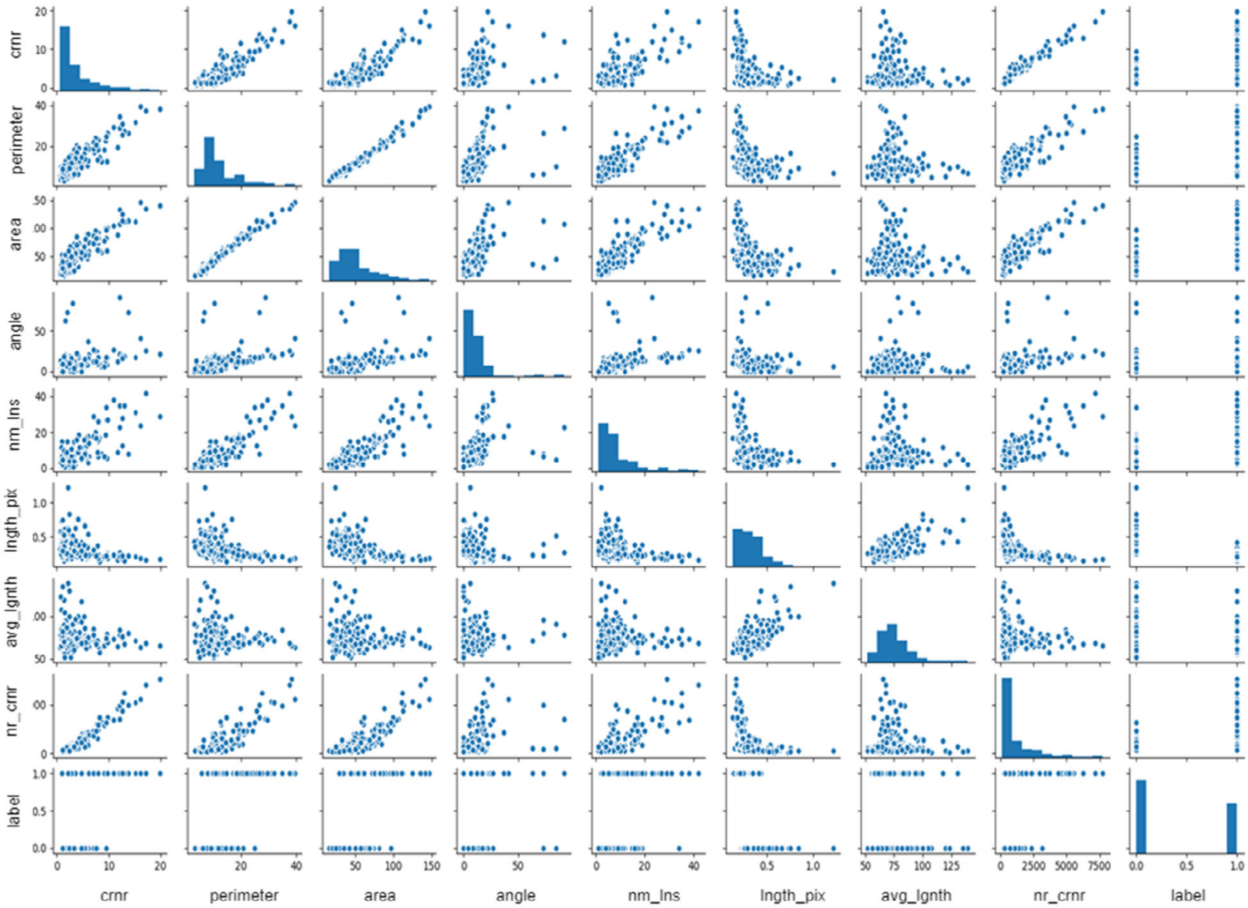

FIGURE 6 Scatter plot of the features

knowledge of the variability or distribution of the data. A boxplot is a graph that shows how the distribution of values in the data is distributed. Figure 10 shows the outcomes of this study's analysis of the classifiers using the 10-fold cross-validation method.

When the training time is considered, Table 2 shows that QDA is better than the other classifiers, while the MLP classifier has the best test time when the training time is considered. The LDA classifier, however, has the dataset's highest accuracy rate. In addition, the most used feature of the algorithm with the highest accuracy rate in the study and its graphic is given in Figure 11. When the figure is examined, it is clear that the number 5 which is called *lngth_pxl* is the most used feature for LDA classifier.

4 | DISCUSSION

It is considered that some contributions have been made in the literature to the recognition of bone fractures. The fact that there are deep learning models for detecting bone fractures in the literature emphasizes the significance of this study. The active use of image processing techniques in the extraction of features obtained from the data used in machine learning algorithms adds a separate innovation to the study. In the study, 12 different machine learning classifiers are used and hyperparameter optimization is performed for the classifiers. In order to ensure the distribution of the data set and the accuracy of the classifiers, the results are obtained using the cross-validation method, and the training and testing times of the classifiers are presented comparatively. By examining the results, it is found that the LDA classifier performs the best among the 12 classifiers. Our study has some limitations. The main problems include the lack of images in the dataset and the lack of labeled data for bone fractures. The use of CT images instead of radiographs in future studies will allow the acquisition of a more comprehensive dataset.

5 | CONCLUSIONS

In this study, an automatic bone fracture detection system based on computer vision techniques and machine

FIGURE 7 Confusion matrix and classificaiton reports of used classifiers

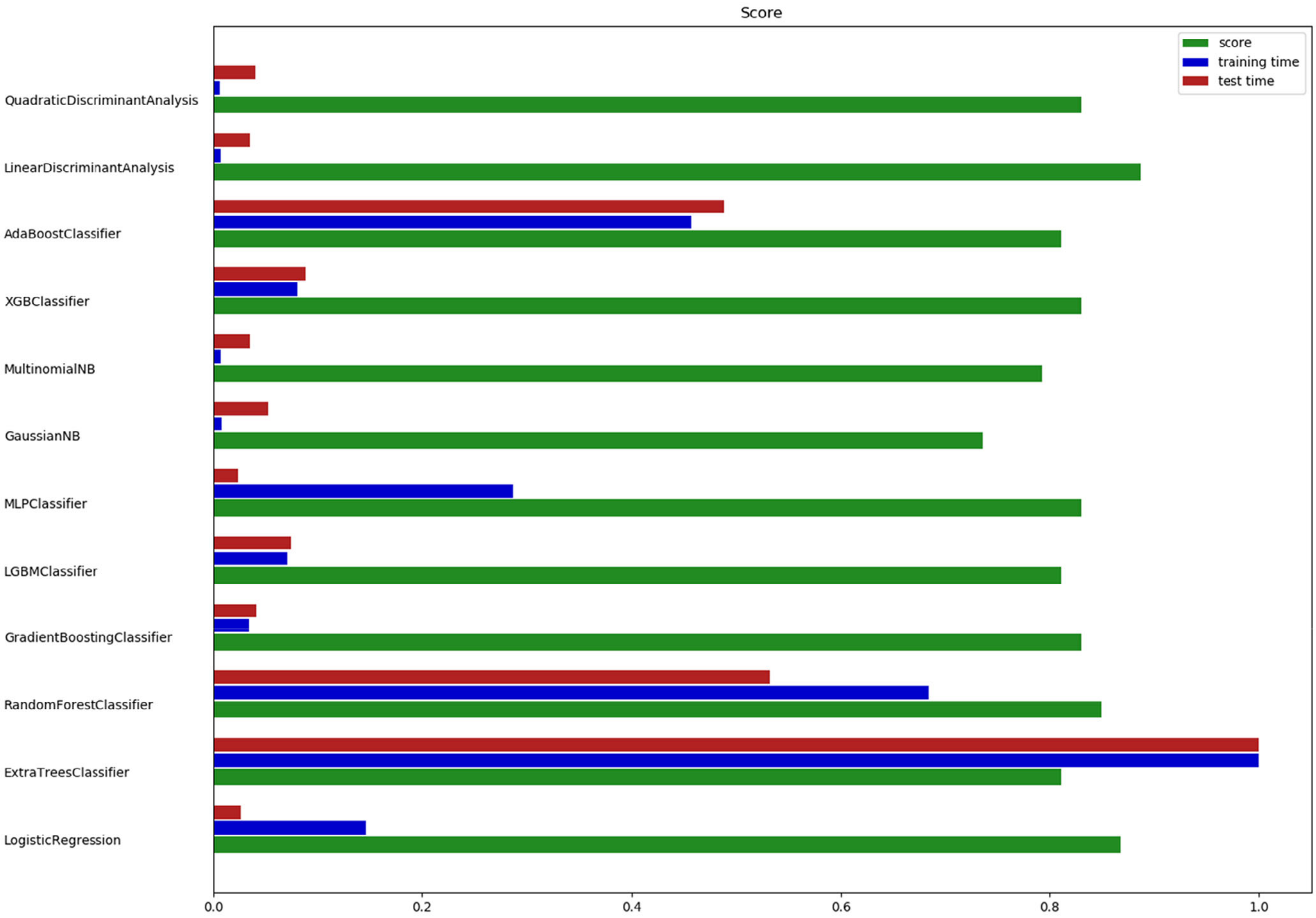

FIGURE 8 Accuracy, training and testing time of used classifiers

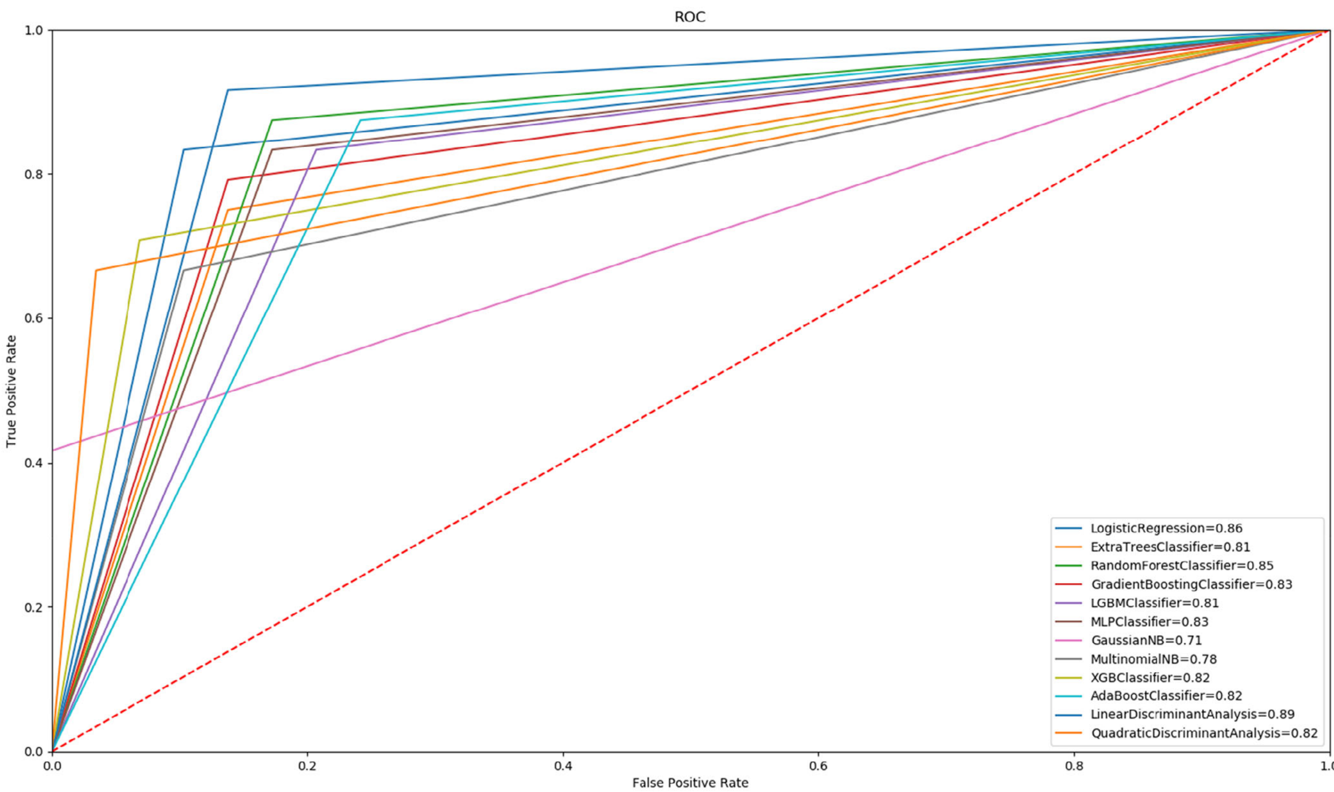

FIGURE 9 ROC graphs of used classifiers

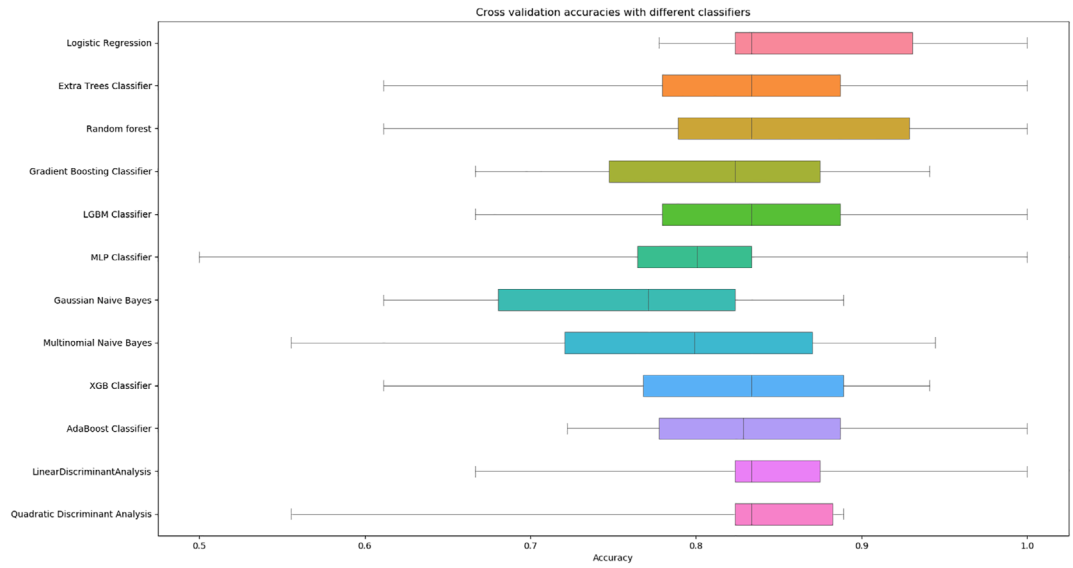

FIGURE 10 Whisker box of used classifiers with 10-fold cross-validation

TABLE 2 Accuracy, training and testing time of used classifiers

Classifier	Accuracy	Training time	Testing time
Gaussian NB	0.7358	0.0076	0.0061
Multinomial NB	0.7924	0.0067	0.0041
Extra trees classifier	0.8113	1.0001	0.1164
LGBM classifier	0.8113	0.0707	0.0086
Ada boost classifier	0.8113	0.4572	0.0568
Gradient boosting classifier	0.8301	0.0342	0.0048
MLP classifier	0.8301	0.2867	0.0027
XGB classifier	0.8301	0.0804	0.0102
Quadratic discriminant analysis	0.8301	0.0066	0.0047
Random forest classifier	0.8490	0.6835	0.0619
Logistic regression	0.8679	0.1454	0.0030
Linear discriminant analysis	0.8867	0.0070	0.0041

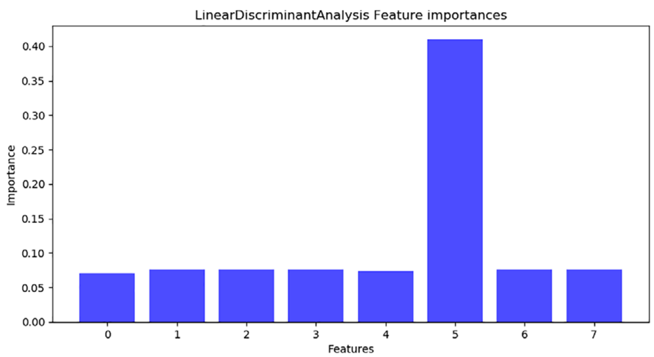

FIGURE 11 Feature importance of Linear discriminant analysis classifier. (0-*crnr*, 1- *perimeter*, 2-*area*, 3-*angle*, 4-*nm_lns*, 5-*lnght_pxl*, 6-*avg_lngth*, 7-*nm_crnr*, 8- *label*)

learning is proposed to improve the automatic detection in the computer-aided diagnosis system. Fully automated fracture detection and classification for specific bone types is an important but very challenging process for both orthopedic surgeons and radiologists. In this study, the X-ray images are processed using a variety of image processing techniques to get them ready for feature extraction. Following the Sobel and Canny edge detection algorithms' processing of the images, Harris corner detection and feature extraction are carried out using the Hough line. The technique of Harris corner detection is particularly useful for identifying bone fracture points. Inputting the detected features into machine learning algorithms is the first step in fracture detection and classification. By adjusting the grid search hyperparameters for the 12 different classifiers used, the effectiveness of the used classifier is improved. With the cross-validation method, machine learning algorithms are examined here for 10-folds, the results are obtained from each algorithms separately. The training and testing times of the used classifiers are also compared. When the results are examined, the LDA classifier yields the best results, with an accuracy rate of 88.67% and an AUC value of 0.89. It is hoped that the information provided in this qualitative review will aid clinicians and researchers in better understanding the current application of machine learning in bone fracture as well as its benefits and drawbacks, especially for those involved in the field of bone health. The accuracy of the model can be improved by using a different deep learning model. A larger dataset needs to be validated to further evaluate the perfromance of the system.

CONFLICT OF INTEREST

The authors declare no conflicts of interest.

DATA AVAILABILITY STATEMENT

The data that support the findings of this study are openly available in Mendeley Data at https://data.mendeley.com/datasets/xbdsnzr8ct/1.

ORCID

Muhammet Emin Sahin https://orcid.org/0000-0001-7729-990X

REFERENCES

1. Beyaz S. A brief history of artificial intelligence and robotic surgery in orthopedics & traumatology and future expectations. *Joint Dis Relat Surg*. 2020;31(3):653-655.
2. Esteva A, Kuprel B, Novoa RA, et al. Dermatologist-level classification of skin cancer with deep neural networks. *Nature*. 2017;542(7639):115-118.
3. Habib N, Hasan M, Reza M, Rahman MM. Ensemble of CheXNet and VGG-19 feature extractor with random forest classifier for pediatric pneumonia detection. *SN Comput Sci*. 2020;1(6):1-9.
4. Olczak J, Fahlberg N, Maki A, et al. Artificial intelligence for analyzing orthopedic trauma radiographs: deep learning algorithms—are they on par with humans for diagnosing fractures? *Acta Orthop*. 2017;88(6):581-586.
5. Şahin ME, Ulutas H, Esra Y. A deep learning approach for detecting pneumonia in chest X-rays. *Avrupa Bilim Ve Teknoloji Dergisi*. 2021;28:562-567.
6. Yaman S, Karakaya B, Erol Y. A novel normalization algorithm to facilitate pre-assessment of Covid-19 disease by improving accuracy of CNN and its FPGA implementation. *Evol Syst*. 2022;1-11. doi:10.1007/s12530-022-09419-3
7. Doegar A. Brain tumor detection and classification using machine learning. *Recent Trends in Communication and Intelligent Systems*. Springer; 2020:227-234.
8. Johri S, Goyal M, Jain S, Baranwal M, Kumar V, Upadhyay R. A novel machine learning-based analytical framework for automatic detection of COVID-19 using chest X-ray images. *Int J Imaging Syst Technol*. 2021;31(3):1105-1119.
9. Asim Y, Raza B, Malik AK, Rathore S, Hussain L, Iftikhar MA. A multi-modal, multi-atlas-based approach for Alzheimer detection via machine learning. *Int J Imaging Syst Technol*. 2018;28(2):113-123.
10. Pranata YD, Wang KC, Wang JC, et al. Deep learning and SURF for automated classification and detection of calcaneus fractures in CT images. *Comput Methods Prog Biomed*. 2019;171:27-37.
11. Li Q, Zhong L, Huang H, et al. Auxiliary diagnosis of developmental dysplasia of the hip by automated detection of Sharp's angle on standardized anteroposterior pelvic radiographs. *Medicine*. 2019;98(52):e18500.
12. Chung SW, Han SS, Lee JW, et al. Automated detection and classification of the proximal humerus fracture by using deep learning algorithm. *Acta Orthop*. 2018;89(4):468-473.
13. Avinash Vishnu V, Divya Prakash J, Swathika R, Sree Sharmila T. Detection and classification of long bone fractures. *Int J Appl Eng Res*. 2015;10(20):18315-18320.
14. Bayram F, Çakıroğlu M. Diffract: Diaphyseal femur fracture classifier system. *Biocybern Biomed Eng*. 2016;36(1):157-171.
15. Tripathi AM, Upadhyay A., Rajput AS, Singh AP, Kumar B. Automatic detection of fracture in femur bones using image processing. Paper presented at: 2017 International Conference on Innovations in Information, Embedded and Communication Systems (ICIIECS). IEEE. 2017;1–5.
16. Basha CMAK, Padmaja M, Balaji GN. Computer aided fracture detection system. *J Med Imag Health Inf*. 2018;8(3):526-531.
17. Guan B, Zhang G, Yao J, Wang X, Wang M. Arm fracture detection in X-rays based on improved deep convolutional neural network. *Comput Electr Eng*. 2020;81:106530.
18. Guan B, Yao J, Zhang G, Wang X. Thigh fracture detection using deep learning method based on new dilated convolutional feature pyramid network. *Pattern Recogn Lett*. 2019;125:521-526.
19. Malik H, Jabbar J, Mehmood H. Wrist Fracture—X-rays. *Mendeley Data*; 2020. doi:10.17632/xbdsnzr8ct.1
20. Balcı K. Üretim Otomasyonunda Görüntü Tabanlı Hata Tanıma Sistemi, Yıldız Teknik Üniversitesi (Master Thesis). 2008.
21. Ding L, Goshtasby A. On the Canny edge detector. *Pattern Recogn*. 2001;34(3):721-725.
22. Canny J. A computational approach to edge detection. *IEEE Trans Pattern Anal Mach Intell*. 1986;6:679-698.
23. Xu Z, Baojie X, Guoxin W. Canny edge detection based on open CV. Paper presented at: 2017 13th IEEE International Conference on Electronic Measurement & Instruments (ICEMI). IEEE. 2017;53–56.
24. Irwin Sobel, History and Definition of the Sobel Operator. 2014.
25. Hough PV. Machine analysis of bubble chamber pictures. Paper presented at: Proceedings of the International Conference on High Energy Accelerators and Instrumentation. 1959;554–556.
26. Harris C, Stephens M. A combined corner and edge detector. *Alvey Vision Conf*. 1988;15(50):10-5244.

27. Rao B. Machine learning algorithms: a review. *Int J Comput Sci Inf Technol*. 2016;7(3):1174-1179. doi:10.21275/ART20203995
28. Sahin ME. Deep learning-based approach for detecting COVID-19 in chest X-rays. *Biomed Signal Process Control*. 2022; 78:103977.
29. Bergstra J, Bengio Y. Random search for hyper-parameter optimization. *J Mach Learn Res*. 2012;13(2):281-305.
30. Klein A, Falkner S, Bartels S, Hennig P, Hutter F. Fast bayesian optimization of machine learning hyperparameters on large datasets. *Artificial Intelligence and Statistics*. PMLR; 2017: 528-536.
31. Witten IH, Frank E. Data mining: practical machine learning tools and techniques with Java implementations. *ACM SIGMOD Rec*. 2002;31(1):76-77.

How to cite this article: Sahin ME. Image processing and machine learning-based bone fracture detection and classification using X-ray images. *Int J Imaging Syst Technol*. 2023;33(3): 853-865. doi:10.1002/ima.22849